The Transition Metal–Carbonyl Bond

ERNEST R. DAVIDSON,* KATHRYN L. KUNZE,† FRANCISCO B. C. MACHADO, AND SUBHAS J. CHAKRAVORTY

Department of Chemistry, Indiana University, Bloomington, Indiana 47405

Received June 1, 1993

Semiempirical theories of bonding in molecules containing transition metals are often merely interpretive. That is, given the experimental fact that a molecule exists and has a particular shape, theory is used to provide a plausible ad hoc justification. Much interpretation of this type uses molecular orbital theory[1] and ascribes bonding effects to orbital mixing. Earlier approaches such as ligand-field theory have been more or less abandoned along with the alternative insights they provided. Modern ab initio methods, on the other hand, have the possibility of being quantitatively predictive. They can be used to study the relative energies of the observed structure and nonobserved plausible alternatives. They can also be used to examine energies along hypothetical steps that allow a partitioning of the binding energy into conceptually interesting, but nonobservable, pieces. A difficulty with many ab initio results, however, is that they merely verify that theory is able to reproduce the experimental facts, and they do not shed additional insight.

In recent years, we have been interested in the bond between a transition metal in its zero oxidation state and a carbonyl with the carbon end next to the metal. This type of bond occurs in many transition metal complexes and in the chemisorption of carbonyl to a metal surface. In particular, we have published calculations[2–9] on $Cr(CO)_6$, $Sc(CO)$, $HCo(CO)_4$, and related species involved in hydroformylation reactions.

Table I summarizes some experimental facts[10] about the simple sequence of molecules $Cr(CO)_6$, $Fe(CO)_5$, and $Ni(CO)_4$. The dissociation energy, per CO, is about the same in these three molecules. All have shapes corresponding to maximum symmetry with linear M–C–O bonds. All obey the 18-electron rule if one electron pair is counted from each CO. In the ligand-field sense, all are near the high-field limit. The d orbital energies are strongly split, and the wave function is dominated by a single closed shell arrangement of the electrons.

Table I. Properties of Some Metal Carbonyl Compounds

	D_e[a]	D_e*[b]	R_{MC}[c]	R_{CO}[c]	ν_{CO}[d]
$Cr(CO)_6$	26[h]	50[h]	1.916[e]	1.140[e]	2112 (a)[j]
					2018 (e)
					1984 (f)
$Fe(CO)_5$	28[h]	51[h]	1.8112[f]	1.1172[f]	2120[h]
			1.8032	1.1333	2042
					2034
					2013 (e)
$Ni(CO)_4$	35[h]	46[h]	1.8172[f]	1.1273[f]	2132 (a)[i]
					2058 (f)
CO				1.1283[g]	2143[g]

[a] Mean bond dissociation energy relative to ground-state atom (kcal/mol). [b] Mean bond dissociation energy relative to promoted atom (kcal/mol). [c] Bond lengths (Å). For $Fe(CO)_5$ the axial distances are on the first line and equatorial distances on the second. The crystal CO distances of $Fe(CO)_5$ and $Ni(CO)_4$ are not corrected for thermal motion. [d] CO stretching transition frequencies (cm^{-1}), $\tilde{\omega}_0$. The average values are 2017 for $Cr(CO)_6$, 2044 for $Fe(CO)_5$, and 2077 for $Ni(CO)_4$. [e] Reference 10c. [f] Reference 10b. [g] Reference 10d. [h] Reference 10a. [i] Reference 10e. [j] Reference 10f. [k] Reference 10g.

The highest occupied molecular orbital (HOMO) of CO is 5σ. This is a lone-pair sp hybrid localized on carbon and pointing away from oxygen. The 5σ orbital extends in space well beyond the molecule and appears to be well suited for forming a coordinate–covalent bond by sharing this electron pair with an empty orbital on the metal. This concept provides a rationalization for the shape and number of ligands in the sequence $Cr(CO)_6$, $Fe(CO)_5$, and $Ni(CO)_4$ which could involve[11]

Ernest R. Davidson was born in Terre Haute, IN, on October 12, 1936. He received his B.S. in chemical engineering from Rose-Hulman Institute in 1958 and his Ph.D. from Indiana University in 1961. After a year as an NSF Postdoctoral Fellow at the University of Wisconsin, Madison, he joined the University of Washington Chemistry Department in 1962. He is now a Distinguished Professor of Chemistry at Indiana University.

Kathryn L. Kunze (deceased, 1991) was born in Paoli, PA, on August 30, 1952. She received her B.S. in chemistry in 1976 from Eastern College, Saint Davids, PA, and her Ph.D. in physical chemistry from Villanova University in 1983. She was a postdoctoral research associate at Texas A & M University from 1984 to 1986 and at Michigan State University from 1987 to 1989. She was a postdoctoral research associate at Indiana University from 1989 to 1991.

Francisco B. C. Machado was born in Barreiras, Brazil, on February 26, 1959. He concluded his B.S. in chemistry in 1981 from São Paulo University, Ribeirão Preto, Brazil. He received his M.S. in 1985 and his Ph.D. in quantum chemistry in 1990 from São Paulo University, São Paulo, Brazil. He is a Research Associate at Instituto de Estudos Avançados-CTA, São José dos Campos, Brazil. Presently he is doing his postdoctoral training at Indiana University.

Subhas J. Chakravorty was born in Pune, India, on July 22, 1960. He received his B.S. in chemistry in 1980 from Fergusson College, Pune, India, and his M.S. in physical chemistry in 1982 and his Ph.D. in quantum chemistry in 1987 from the University of Poona, Pune, India. He did postdoctoral work at IBM, Kingston, NY, from 1987 to 1990. He presently is continuing his postdoctoral training at Indiana University.

* Author to whom correspondence should be addressed.
† Deceased, March 28, 1991.

(1) Throughout this Account we will use "MO theory" to denote a model where the wave function consists of a single Slater determinant built from molecular orbitals. These MOs may be determined from either ab initio Hartree–Fock calculations or semiempirical models.

(2) Kunze, K. L.; Davidson, E. R. *J. Phys. Chem.* **1992**, *96*, 2129.
(3) Frey, R. F.; Davidson, E. R. *J. Chem. Phys.* **1989**, *90*, 5555.
(4) Frey, R. F.; Davidson, E. R. *J. Chem. Phys.* **1989**, *90*, 5541.
(5) Davidson, E. R. In *The* Challenge *of d and f Electrons: Theory and Computation*; Salahub, D. R., Zerner, M. C., Eds.; ACS Symposium Series 394; American Chemical Society: Washington, DC, 1989; pp 153–164.
(6) Antolovic, D.; Davidson, E. R. *J. Am. Chem. Soc.* **1987**, *109*, 977.
(7) Antolovic, D.; Davidson, E. R. *J. Am. Chem. Soc.* **1987**, *109*, 5828.
(8) Antolovic, D.; Davidson, E. R. *J. Chem. Phys.* **1988**, *88*, 4967.
(9) Machado, F. B. C.; Davidson, E. R. *J. Phys. Chem.* **1993**, *97*, 4397.
(10) (a) Ziegler, T.; Tschinke, V.; Ursenbach, C. *J. Am. Chem.* **1987**, *109*, 4825. (b) Braga, D.; Grepioni, F.; Orpen, A. G. *Organometallics* **1993**, *12*, 1481. (c) Rees, B.; Mitschler, A. *J. Am. Chem. Soc.* **1976**, *98*, 7918. (d) Huber, K. P.; Herzberg, G. *Constants of Diatomic Molecules*; Van Nostrand-Reinhold: New York, 1979. (e) Jones, L. H.; McDowell, R. S.; Goldblatt, M. *J. Chem. Phys.* **1979**, *70*, 3224. (f) Jones, L. H. *Inorg. Chem.* **1976**, *15*, 1244. (g) Jones, L. H.; McDowell, R. S.; Goldblatt, M.; Swanson, B. I. *J. Chem. Phys.* **1972**, *57*, 2050.
(11) Kimball, G. E. *J. Chem. Phys.* **1940**, *8*, 188.

0001-4842/93/0126-0628$04.00/0

empty sp^3d^2, sp^3d, and sp^3 hybrid orbitals, respectively, on the metal acting as electron pair acceptors. Semiempirical estimates of the bond lengths and vibrational frequencies resulting from this type of bonding show that, unfortunately, this explanation cannot account for the observed properties. This σ donor view of bonding was replaced in about 1950 by the Dewar–Chatt–Duncanson model.[12] In this view most of the bond energy is ascribed to "π back-bonding" in which the highest occupied atomic orbitals (HOAO) of the metal mix with the lowest empty molecular orbital (LUMO) of CO. In the semiempirical approach, the LUMO is the empty π antibonding orbital of CO, denoted as $2\pi^*$. This mixing is ascribed to "overlap" of a filled metal d orbital and the empty CO $2\pi^*$ orbital.

There is a technical flaw in this vocabulary for describing the effect of orbital mixing. In ab initio calculations, it is possible to introduce the CO orbitals, including $2\pi^*$, into a calculation on the free metal atom without actually introducing the CO nuclei and electrons. The overlap with the metal orbitals would be the same in this case, but any energy lowering would be regarded as an error (called "basis set superposition error" or BSSE). If the metal orbitals were already optimal, no further improvement would be possible. Hence the true energy-lowering effect of HOMO–LUMO mixing is not due to "overlap" but is driven by the perturbing potential of the associated ligand nuclei and electrons. The confusion arises in the semiempirical literature because the HOMO–LUMO mixing matrix element of the perturbing potential is assumed to be proportional to the overlap.

Several papers have appeared during the last few years evaluating the σ donation and π back-bonding energies by ab initio methods.[13] While the details of these papers differ, they all agree that π back-bonding is more important than σ donation. Further, the metal 4s and 4p orbitals play only a small role in bonding even in $Ni(CO)_4$ where there are no empty d orbitals. They also agree that the π back-bonding energy is of the same order of magnitude as the observed bond energy. Early Xα density functional calculations[14] had reached the opposite conclusion and claimed that the bonding was mostly σ donation, but more recent LSDA density functional calculations[10a] ascribe most of the energy to π back-bonding. Nevertheless, as we will explain below, many effects not associated with covalency contribute to the observed bond strength.

In order to arrive at a more comprehensive view, it is important to identify all of the contributions to the bond energy which are large enough to be significant. We will focus particularly on $Cr(CO)_6$, but the results are similar for other metal carbonyls. The total bond energy of a metal carbonyl is defined by

$$M + nCO \rightarrow M(CO)_n \qquad \Delta E = -D_0 \qquad (1)$$

where M is a gas-phase atom in its ground state and CO and $M(CO)_n$ are in their ground vibrational and rotational states. For convenience it is common to adjust the experimental D_0 for the estimated zero-point vibrational energies and focus the discussion on

$$M + nCO(R_e) \rightarrow M(CO)_n(X_e) \qquad \Delta E = -D_e \quad (2)$$

where R_e is the bond length of CO at its free, gas-phase equilibrium geometry and X_e symbolizes the structural parameters of the complex at its equilibrium structure.

It is helpful to split this reaction into several steps. In most cases, the effective electron configuration of the metal in the complex is different from that of the ground state of the free atom, so we can consider the promotion energy for putting the atom into the desired electron configuration.

$$M \rightarrow M^* \qquad \Delta E = P_M \qquad (3)$$

It is also useful to consider separately the promotion energy required to distort all of the ligands into the shape they have in the complex.

$$CO(R_e) \rightarrow CO(X_e) \qquad \Delta E = P_{CO} \qquad (4)$$

We can then imagine assembling these prepared fragments into the final complex. In this Account we have chosen to split that step into two parts. First we imagine assembling all the ligands into an empty cage of the correct final shape.

$$nCO(X_e) \rightarrow (CO)_n(X_e) \qquad \Delta E = P_{cage} \qquad (5)$$

Then we imagine inserting the prepared atom into the center of this cage.

$$M^* + (CO)_n(X_e) \rightarrow M(CO)_n(X_e) \qquad \Delta E = E_{insert} \quad (6)$$

We can then examine the energies involved in each

(12) (a) Hellmann, H. *Dokl. Akad. Nauk SSSR* **1939**, *24*, 549. (b) Pauling, L. *Acta Crystallogr.* **1968**, *B24*, 978. (c) Pauling, L. *The Nature of the Chemical Bond*; Cornell University Press: Ithaca, 1948; p 251. (d) Pauling, L. *J. Chem. Soc.* **1948**, 1461. (e) Dewar, J. S. *Bull. Soc. Chim. Fr.* **1951**, *18*, c79. (f) Chatt, J.; Duncanson, L. A. *J. Chem. Soc.* **1953**, 2939. (g) Chatt, J. *J. Chem. Soc.* **1949**, 3340. (h) Chatt, J.; Wilkins, R. G. *J. Chem. Soc.* **1952**, 2622. (i) Craig, D. P.; Maccoll, A.; Nyholm, R. S.; Orgel, L. E.; Sutton, L. E. *Trans. Faraday Soc.* **1954**, 333. (j) Craig, D. P.; Maccoll, A.; Nyholm, R. S.; Orgel, L. E.; Sutton, L. E. *J. Chem. Soc.* **1954**, 332. (k) Sutton, L. E. *J. Chem. Educ.* **1960**, *37*, 498. (l) Caulton, K. G.; Fenske, R. F. *Inorg. Chem.* **1968**, *7*, 1273. (m) Lichtenberger, D. L.; Fenske, R. F. *Inorg. Chem.* **1976**, *15*, 2015. (n) Lichtenberger, D. L.; Kellogg, G. E. *Acc. Chem. Res.* **1987**, *20*, 379. (o) Fenske, A. K.; Cotton, F. A.; Wilkinson, G. *J. Am. Chem. Soc.* **1957**, *79*, 2044. (p) Beach, N. A.; Gray, H. B. *J. Am. Chem. Soc.* **1968**, *90*, 5713. (q) Gray, H. B.; Beach, N. A. *J. Am. Chem. Soc.* **1963**, *85*, 2922. (r) Hoffmann, R.; Chen, M. M. L.; Thorn, D. L. *Inorg. Chem.* **1977**, *16*, 503. (s) Schilling, B. E. R.; Hoffmann, R. *J. Am. Chem. Soc.* **1979**, *101*, 3456.

(13) See, for example: (a) Bauschlicher, C. W.; Bagus, P. S. *J. Chem. Phys.* **1984**, *81*, 5889. (b) Bauschlicher, C. W.; Pettersson, L. G. M.; Siegbahn, P. E. M. *J. Chem. Phys.* **1987**, *87*, 2129. (c) Bauschlicher, C. W.; Langhoff, S. R.; Barnes, L. A. *Chem. Phys.* **1989**, *129*, 431. (d) Bauschlicher, C. W. *J. Chem. Phys.* **1986**, *84*, 260. (e) Bauschlicher, C. W.; Bagus, P. S.; Nelin, C. J.; Roos, B. O. *Chem. Phys.* **1986**, *85*, 354. (f) Barnes, L. A.; Rosi, M.; Bauschlicher, C. W. *J. Chem. Phys.* **1991**, *94*, 2031. (g) Barnes, L. A.; Rosi, M.; Bauschlicher, C. W. *J. Chem. Phys.* **1990**, *93*, 609. (h) Barnes, L. A.; Bauschlicher, C. W. *J. Chem. Phys.* **1989**, *91*, 314. (i) Blomberg, M. R. A.; Brandemark, U. B.; Siegbahn, P. E. M.; Wennerberg, J.; Bauschlicher, C. W. *J. Am. Chem. Soc.* **1988**, *110*, 6650. (j) Hall, M. B.; Fenske, R. F. *Inorg. Chem.* **1972**, *11*, 1620. (k) Sherwood, D. E.; Hall, M. B. *Inorg. Chem.* **1979**, *18*, 2325. (l) Sherwood, D. E.; Hall, M. B. *Inorg. Chem.* **1980**, *19*, 1805. (m) Williamson, R. L.; Hall, M. B. *Int. J. Quantum Chem.* **1987**, *21S*, 503. (n) Hillier, I. H.; Saunders, V. R. *Mol. Phys.* **1971**, *22*, 1025. (o) Hillier, I. H.; Saunders, V. R. *J. Chem. Soc., Chem. Commun.* **1971**, 642. (p) Ford, P. C.; Hillier, I. H. *J. Chem. Phys.* **1984**, *80*, 5664. (q) Ford, P. C.; Hillier, I. H.; Pope, S. A.; Guest, M. F. *Chem. Phys. Lett.* **1983**, *102*, 555. (r) Cooper, G.; Green, J. C.; Payne, M. P.; Dobson, B. R.; Hillier, I. H. *Chem. Phys. Lett.* **1986**, *125*, 97. (s) Cooper, G.; Green, J. C.; Payne, M. P.; Dobson, B. R.; Hillier, I. H. *J. Am. Chem. Soc.* **1987**, *109*, 3836. (t) Guest, M. F.; Hillier, I. H.; Vincent, M.; Rosi, M. *J. Chem. Soc., Chem. Commun.* **1986**, 438. (u) Moncrieff, D.; Ford, P. C.; Hillier, I. H.; Saunders, V. R. *J. Chem. Soc., Chem. Commun.* **1983**, 1108. (v) Smith, S.; Hillier, I. H.; von Niessen, W.; Guest, M. F. *Chem. Phys.* **1989**, *135*, 357. (w) Vanquickenborne, L. G.; Verhulst, J. *J. Am. Chem. Soc.* **1987**, *109*, 4825. (x) Pierfoot, K.; Verhulst, J.; Verbeke, P.; Vanquickenborne, L. G. *Inorg. Chem.* **1989**, *28*, 3059. (y) Yamamoto, S.; Kashiwagi, H. *Chem. Phys. Lett.* **1993**, *205*, 306 (z) Blomberg, M. R. A.; Siegbahn, P. E. M.; Lee, T. L.; Rendell, A. P.; Rice, J. E. *J. Chem. Phys.* **1991**, *95*, 5898.

(14) Johnson, J. B.; Klemperer, W. G. *J. Am. Chem. Soc.* **1977**, *99*, 7132.

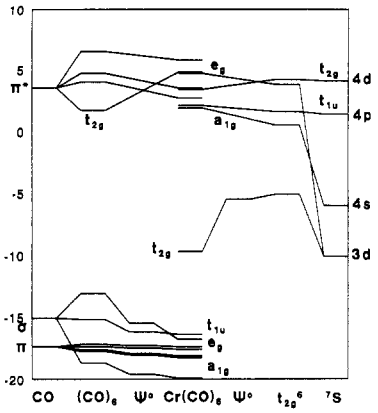

Figure 1. Orbital energies (eV) after various steps in forming $Cr(CO)_6$.

step. Note that any orbital mixing between the metal and the CO takes place only in the final step. The dissociation energy can be found as the sum of the energies of these steps:

$$-D_e = P_M + nP_{CO} + P_{cage} + E_{insert} \quad (7)$$

Only the final step lowers the energy; the rest are promotion steps needed to get the fragments as nearly as possible into the form they have in the complex.

The molecular orbital description of these complexes has the metal in a low-spin state with all of the valence electrons paired up and placed in d orbitals. Thus, although Cr is normally in a d^5s^1 ^7S state as a free atom, it is effectively in a t_{2g}^6 $^1A_{1g}$ configuration in the complex. This spin-pairing promotion is analogous to, but has the opposite effect of, the spin-unpairing promotion of the carbon atom which allows carbon to form four covalent bonds. For coordination to Lewis bases, the metal electrons are first paired to generate as many empty "electron-pair acceptor" orbitals as needed. This is true in these complexes even though donation of electron pairs to these acceptor orbitals is not the primary bonding mechanism. Essentially, even though these empty–filled σ donations are not very stabilizing, the corresponding filled–filled repulsions that would result if the metal orbitals were not emptied would be strongly destabilizing.

Figure 1 shows an orbital energy diagram, based on ab initio orbital energies, along this sequence of steps in the formation of $Cr(CO)_6$ from ^7S Cr and six CO molecules. The orbital energy for an orbital fully occupied in the ground state of the molecule is approximately the negative of the ionization energy. In orbital energy diagrams based on extended Hückel theory (EHT), which are more familiar in the inorganic literature, the orbital energy of an orbital empty in the ground state is defined to be approximately the negative of the ionization energy in an excited state of the neutral molecule in which this orbital is occupied. With the EHT definition, differences of orbital energies are approximate excitation energies. Ab initio orbital energies for empty orbitals are defined quite differently. In Figure 1, the vacant orbital energies are to be interpreted as the negatives of electron affinities. Energies of partially occupied orbitals are the negatives of averages of corresponding electron affinities and ionization energies. Differences of ab initio orbital energies have no simple relation to excitation energies.

Table II. Numerical Hartree–Fock Excitation Energies[a]

	$d^ns^2 \rightarrow d^{n+1}s$		d^{n+2}		d^nsp		
	calcd	exptl	calcd	exptl	calcd	exptl	n
Sc	8105	11 520	36 053	33 764	7704	15 672	1
Ti	4357	6556	34 321	28 773	7478	15 877	2
V	1001	2112	26 366	20 202	7251	16 361	3
Cr	−10 219	−7751	46 421	27 647	7528	17 220	4
Mn	26 840	17 052	73 836	44 979	8601	18 402	5
Fe	14 494	6929	60 178	32 874	8788	19 351	6
Co	12 328	3483	56 846	27 497	12 800	23 612	7
Ni	10 289	205	44 147	14 729	15 591	25 754	8
Cu	−2998	−11 203			16 700	27 816	9
Zn					21 315	32 311	10

[a] ΔSCF energies (cm^{-1}) between the lowest LS multiplets, table taken from ref 5.

Also, these orbital energies are determined self-consistently. Thus when the atomic occupation is changed, the orbital energies may change dramatically with no change in the shape of the orbital. In the d^5s^1 configuration of Cr with atomic spherical symmetry, the d orbitals are degenerate; but in the t_{2g}^6 configuration computed in O_h symmetry, the two empty 3d orbitals with symmetry e_g are assigned a much higher energy than the three filled 3d orbitals of t_{2g} symmetry because the electron affinity for adding another d electron to e_g is very different from the energy to remove an existing electron from t_{2g}. Figure 1 also shows many empty orbitals with positive orbital energies. Within the MO approximation, an electron placed in one of these orbitals would auto-ionize. Molecular orbital theory using orbitals determined for the neutral molecule is very inaccurate for anions, and in this case it predicts that no stable anion exists. If a complete basis set were used, these empty orbitals would disappear and be replaced by a continuum beginning at zero orbital energy. Antibonding orbitals like $2\pi^*$ on CO appear only when EHT theory or small basis sets are used. No well-defined energy can be assigned to this orbital, and the orbital would not appear in a calculation with a complete basis set.

Another important fact about ab initio orbital energies is that there is no direct connection with the total energy of the atom or molecule. Examination of the complete list of orbital energies shows, in fact, that the inner core energies change by as much as the valence orbitals even though the core orbitals themselves are virtually unchanged in shape. As is well-known in photoelectron spectroscopy, the ionization energy of the core electrons is strongly affected by the electrostatic potential generated by the valence electrons. During the steps in forming $Cr(CO)_6$, the sum of the orbital energies changes by an order of magnitude more than the total energy. Not all effects which lower the HOMO orbital energy contribute directly to an increased dissociation energy.

Table II shows the experimental excitation energies of a few transition metal atoms compared to the results of numerical Hartree–Fock calculations. From this table, two important conclusions are obvious. First, the promotion energy is a large number and must be considered in any qualitative explanation of the bond strength. Table I compares the bond strengths D_e with what they would be if they were measured relative to the promoted atom. Clearly, the promotion energy significantly weakens the bond. The second obvious

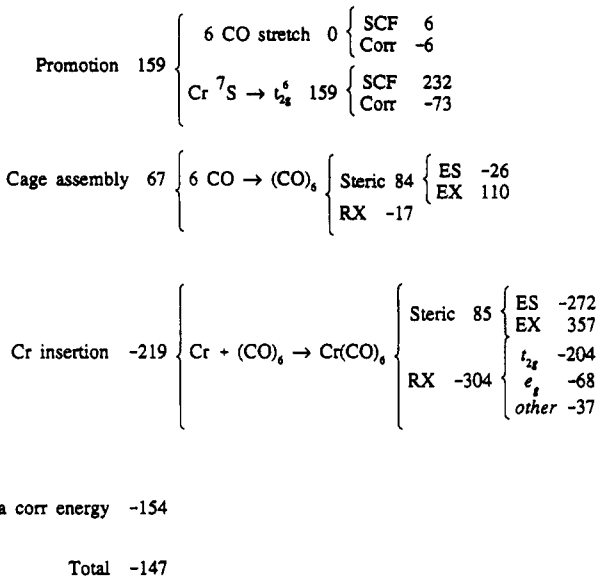

Figure 2. Energetics of various steps in $Cr(CO)_6$ formation (kcal/mol) showing SCF-MO, electron correlation, electrostatic (ES), exchange repulsion (EX), and relaxation (RX) contributions.

conclusion from Table II is that the Hartree–Fock excitation energy is a very poor estimate of the true excitation energy. Consequently, MO theory for D_e will not be very accurate since promotion of the Cr is an important step in the bond formation process. Also, the $d^n sp$ states are consistently calculated too low in energy and d^{n+2} too high in energy. This leads to the wrong configuration of the central metal in some Sc and Co complexes.

As shown in Figure 2, the promotion energy of Cr is calculated to be 232 kcal/mol using Hartree–Fock theory. The error in the Hartree–Fock energy is defined to be the "electron correlation energy". This can be calculated by configuration interaction or coupled cluster methods for open shell systems. Density functional theory and perturbation theory can be used for closed shell molecules (and with caution for open shell atoms). It is even more difficult to define the electron correlation for a hypothetical situation like t_{2g}^6 which lacks atomic symmetry. Nevertheless, calculations and empirical estimates based on extrapolating errors like those in Table II agree that P_M is approximately 159 kcal/mol. The theoretical calculation of these numbers has been done in the full molecular basis set so that no energy stabilization will be caused by BSSE effects. Note that P_M is almost exactly equal to D_e for $Cr(CO)_6$, so D_e^* is about double D_e.

Except for the atomic promotion step, the electron configuration changes very little through the remaining steps, and one might hope that MO theory would be adequate as a semiquantitative model of

$$-D_e^* = -(D_e + P_M) = nP_{CO} + P_{cage} + E_{insert} \quad (8)$$

We will see that this is not so.

There is a small energy effect, P_{CO}, associated with stretching the CO molecules. The true value of P_{CO} can easily be estimated from $^1/_2 k_e(X_e - R_e)^2$, using the experimental force constant, to be less than 1 kcal/mol. MO theory gives a rather poor estimate of R_e. As a result, MO theory gives too large a value for P_{CO} based on experimental bond lengths and the MO energy increase must be nearly canceled by the electron correlation correction.

In the $Cr(CO)_6$ complex, the neighboring C–C distances are less than the sum of the van der Waals radii. Formation of the $(CO)_6$ cage without the Cr atom leads to "steric repulsion" from these nonbonded contacts. The in-phase combination of the 5σ CO orbitals is strongly bonding between adjacent CO molecules and gives an a_{1g} molecular orbital for the cage of much lowered orbital energy. The t_{1u} combination involves the difference of 5σ orbitals on axially opposite CO molecules so is nonbonding in the empty cage. The e_g combination has the same sign pattern as the metal $3d_{z^2}$ and $3d_{x^2-y^2}$ e_g orbitals and is antibonding between adjacent CO molecules in the empty cage. The filled 1π and empty $2\pi^*$ CO orbitals correlate with t_{1g}, t_{2g}, t_{1u}, and t_{2u} orbitals of the cage. Among the $2\pi^*$ virtual orbitals, the t_{2g} combination is bonding between adjacent CO molecules and is stabilized by cage formation. This makes it a much better electron acceptor orbital than the $2\pi^*$ orbital of an isolated CO.

The net repulsion between the CO molecules is not obvious from the behavior of the orbital energies. The total energy is most easily analyzed by the Morokuma energy partitioning[15] designed for studies of van der Waals and hydrogen-bonded complexes. In this scheme the electrostatic energy, ES, is defined as the classical Coulomb's law energy calculated with the charge distributions of the unperturbed molecules. For this cage formation ES is −26 kcal/mol. Next, the steric energy ΔE° is defined as the change in energy if the cage is assembled keeping the molecular orbitals unchanged from the free fragments. This gives 84 kcal/mol repulsion. While this quantity is commonly called the "steric" energy in the theoretical literature.[10a] it is not clear whether this definition conforms to the looser use of this phrase in the inorganic literature. Since the steric energy includes the electrostatic energy, this ES can be subtracted to give the "exchange repulsion", EX, which is 110 kcal/mol in this example. Most of the exchange repulsion is due to increased kinetic energy caused by the Pauli exclusion principle. The MO wave function formed from the nonorthogonal fragment orbitals is identical to the MO wave function in which these occupied orbitals have been orthogonalized. When the orbitals are orthogonal, they have additional nodes which increase their average kinetic energy and the total kinetic energy is just the sum of the orbital kinetic energies for orthogonal orbitals. The wave function using nonorthogonal orbitals has the same average kinetic energy, of course, but the value is not simply related to the orbital kinetic energies. Orthogonalization of the fragment orbitals could be done in many ways. In order to obtain meaningful orbital energies, we always choose the orthogonal orbitals so the Fock operator formed from these orbitals is diagonal in this basis of occupied fragment orbitals.

(15) (a) Morokuma, K. *J. Chem. Phys.* **1971**, *55*, 1236. (b) Morokuma, K. *Acc. Chem. Res.* **1977**, *10*, 294. (c) Morokuma, K.; Kitaura, K. *Chemical Applications of Atomic and Molecular Electrostatic Potentials*; Politzer, P., Truhlar, D. G., Eds.; Plenum: New York, 1981; p 215. (d) Kitaura, K.; Sakaki, S.; Morokuma, K. *Inorg. Chem.* **1981**, *20*, 2292. (e) Kitaura, K.; Morokuma, K. *Int. J. Quantum Chem.* **1976**, *10*, 325. (f) Nagase, S.; Fueno, T.; Yamabe, S.; Kitaura, K. *Theor. Chim. Acta* **1978**, *49*, 309. (g) Umeyama, H.; Morokuma, K. *J. Am. Chem. Soc.* **1977**, *99*, 1316. (h) Yamabe, S.; Morokuma, K. *J. Am. Chem. Soc.* **1975**, *97*, 4458.

The final step in partitioning the cage formation energy consists of allowing the orbitals to relax to the optimum orbitals for the cage. This gives an associated relaxation energy, RX, of −17 kcal/mol. Insertion of the metal into this cage will also introduce additional basis functions at the cage center. In order to prevent ascribing any bond energy to this improvement of the cage wave function, the Cr basis functions were included during the relaxation step and during the calculation of each CO molecule. In particular, this means that no energy effects are associated with delocalization of CO cage electrons into metal orbitals when the metal is not actually present. The MO estimate of the cage fromation energy is 67 kcal/mol. There should be an additional energy contribution to the cage energy from electron correlation, but this has been included in the extramolecular electron correlation and has not been evaluated separately.

Finally, we can examine the bonding that takes place when the promoted Cr atom is inserted into the $(CO)_6$ cage. This again can be separated using the Morokuma analysis into a steric component and an orbital mixing (relaxation) component. The steric component is computed using the cage and promoted metal occupied orbitals. Figure 1 shows the orbital energies (labeled as Ψ°) after this step. Notice that most of the orbital energy lowering of the cage orbitals already occurs in this step, so this energy lowering is due to the metal's electrostatic potential and not to orbital mixing. The metal 3d t_{2g} orbital energy by contrast is nearly unchanged in the steric step. In spite of the stabilization of the orbital energies shown in Figure 1, the steric energy is repulsive by 85 kcal/mol. This can be broken down into −272 kcal/mol of electrostatic attraction and 357 kcal/mol of exchange repulsion. Both of these numbers are very large compared to the value of D_e and deserve some comment. The cage and the atom both have high symmetry and zero charge, so the long-range electrostatic attraction should be very small. The large value obtained here is due to the penetration of the 5σ electrons into the metal 3spd shell so that these 5σ electrons are not fully shielded from the highly charged metal nucleus. The large exchange repulsion is caused by this same penetration. In this case, the filled a_{1g} and t_{1u} cage orbitals overlap the filled 3s and 3p orbitals of the metal giving a large filled–filled interaction due to the increased kinetic energy. This is evident in the orbital energy diagram where the e_g cage orbital, which does not overlap any filled metal orbital, is more stabilized than the a_{1g} and t_{1u} orbitals, in which electrostatic stabilization is competing with exchange repulsion.

The relaxation of the orbitals in this insertion step has been the focus of most discussions of the bonding in this complex. The vocabulary of HOMO–LUMO mixing focuses on this relaxation step, and consequently, much of the ab initio literature has also focused on this part of the energy. During the relaxation step, all of the orbitals change to their final optimum form. Figure 1 shows that the largest orbital energy change, by far, is associated with the metal t_{2g} orbital in agreement with semiempirical expectations. The cage e_g orbital energy undergoes a smaller stabilizing change, and the changes in the orther orbital energies shown in Figure 1 are small. Figures 3 and 4 show contour maps

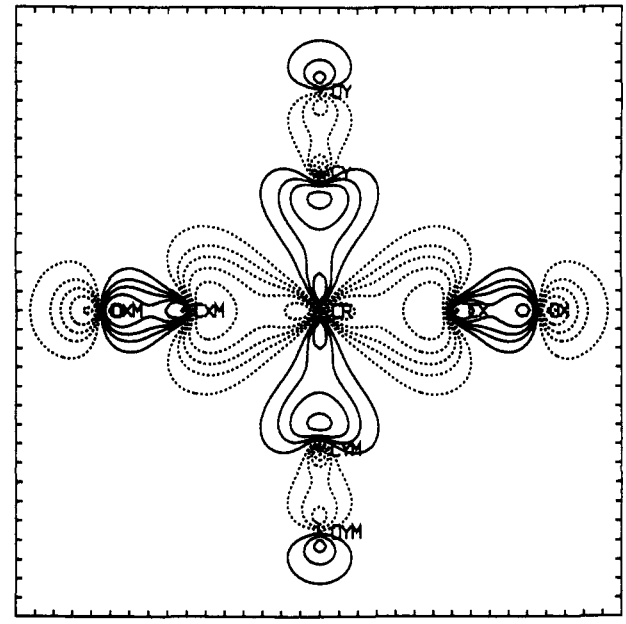

Figure 3. A contour map of the 5σ e_g x^2-y^2 orbital of $Cr(CO)_6$.

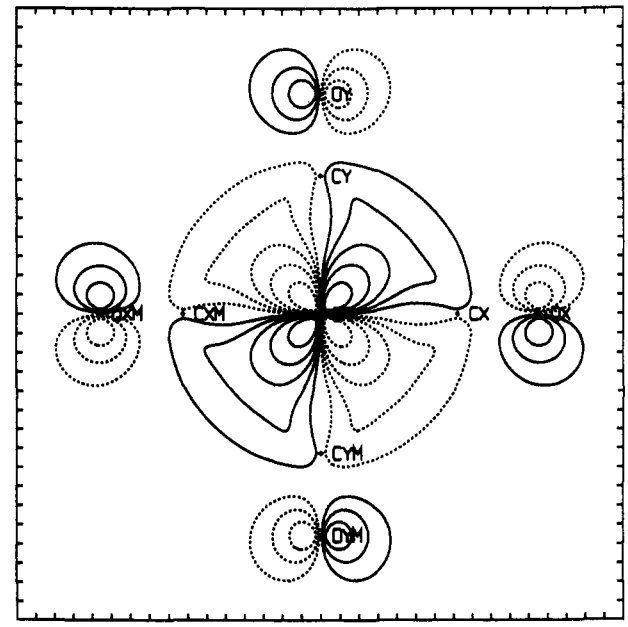

Figure 4. A contour map of the 3d t_{2g} xy orbital of $Cr(CO)_6$.

of the e_g and t_{2g} orbitals after relaxation. The e_g orbital clearly acquires some metal 3d e_g character. The metal t_{2g} orbital change is not so clearly what was expected. Most noticeably this orbital becomes generally more diffuse compared with the free atom 3d orbital shown in Figure 5. This diffuseness can be regarded as the result of mixing with the empty 4d t_{2g} metal orbital and is caused by increased shielding of the 3d electrons from the Cr nuclear charge by the CO 5σ electrons which have penetrated into the 3spd shell of the Cr. This same shielding effect drives the mixing of the metal t_{2g} orbital with the empty cage $2\pi^*$ t_{2g} orbital. Clearly the 3d t_{2g} orbital in the t_{2g}^6 metal configuration is the most polarizable orbital in the complex and responds with rather large changes to perturbations.

Partitioning of the total energy improvement into a unique piece assigned to each orbital is not possible. Several schemes have been suggested in the literature. Some of these have a leftover nonadditive piece ascribed to "synergistic" effects. Some avoid a synergistic term

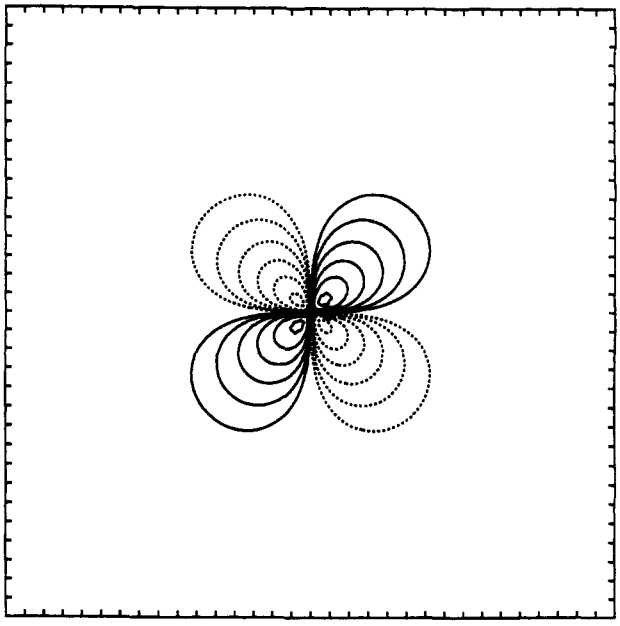

Figure 5. The $3d_{xy}$ orbital of the Cr atom in the 3d t_{2g}^6 configuration.

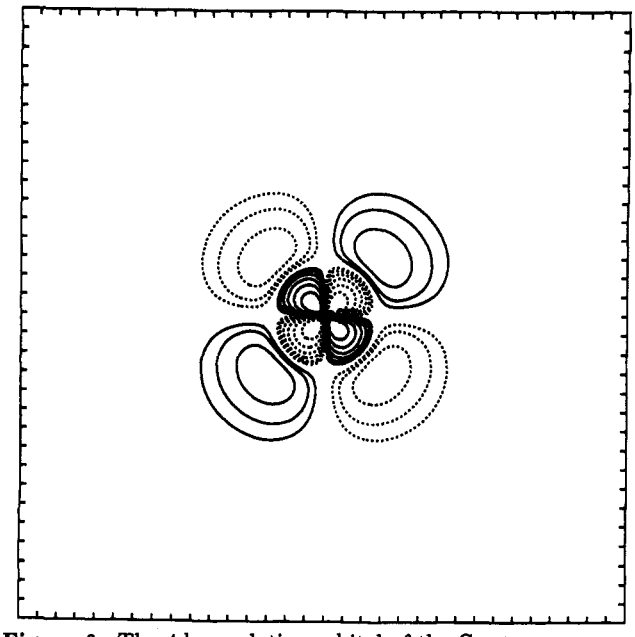

Figure 6. The 4d correlating orbital of the Cr atom.

by allowing the orbitals to relax sequentially (in an arbitrary order) and calculating the energy improvement in each step. Other schemes focus on polarization (mixing of orbitals on the same fragment) compared with charge transfer (mixing of filled orbitals on one fragment with empty orbitals on another fragment). We have examined several such procedures in a previous paper.[2] All methods agree that the 3d t_{2g} relaxation is the dominant effect, so it makes little difference which method is used. In the present paper, we choose to base the partitioning on an interesting identity that assigns a part of the total relaxation energy to each orbital with no synergistic term. If we consider the average of the Fock operators, F_{av}, for Ψ° and the final relaxed Ψ, then the relaxation energy can be written exactly as

$$RX = \sum(\langle\phi|F_{av}|\phi\rangle - \langle\phi^\circ|F_{av}|\phi^\circ\rangle) \qquad (9)$$

That is, the relaxation energy is exactly the sum of the changes in the orbital energy between the final relaxed and initial unrelaxed orbitals provide the average Fock operator is used. Another advantage of this definition is that none of the energy improvement is assigned to orbitals which do not change shape. As shown in Figure 2, this ascribes −204 kcal/mol to the relaxation of the 3d t_{2g} orbital, −68 kcal/mol to the 5σ e_g orbital, and −37 kcal/mol to all the others.

It will be noticed that the total energy change to this point is still repulsive by 7 kcal/mol. That is, the orbital energy mixing in the insertion step is not enough to compensate for all of the promotion and steric energy. Consequently, the MO model cannot actually predict that this molecule exists, let alone give a reasonable estimate of the bond energy. Reliable calculation of the electron correlation energy change upon forming a molecule of this size has only recently become possible. Calculation on $Cr(CO)_6$ gives −154 kcal/mol for this extra molecular correlation.[9] When this is added to the other energy terms, a reasonable estimate of the total bond energy is obtained. Since this last term is of the same magnitude as the bond energy, development of a correct qualitative model of bonding requires development of a vocabulary for describing this part of the energy.

As the phrase "electron correlation" implies, this energy is the improved energy found by describing the detailed ways in which the electron positions are correlated.[9] For the metal promotion energy, for example, the electrons in the 3d t_{2g}^6 configuration have their positions strongly correlated. A large part of this is described in the wave function by adding other configurations in which two of these electrons of opposite spin are placed in a higher energy d orbital of the same size as the 3d but with an additional radial node through the region of high density. A contour map of this correlating "4d" orbital is shown in Figure 6. This promotion causes the electron positions to be correlated so that there is increased probability of finding the electrons on opposite sides of this radial node, and decreased probability of finding them on the same side. This effect is much less important in the d^5s ^7S state, so this correlation reduces the computed promotion energy.

The radial correlation just described persists in the complex, but its magnitude increases only slightly, so it does not make a major contribution to the extra correlation energy. In the complex, this is described by placing two of the t_{2g} electrons in the second t_{2g} orbital shown in Figure 7. While this looked like a 4d orbital for the free atom, it looks more like the cage $2\pi^*$ t_{2g} orbital for the complex. Hence, several authors have noted the importance of $3d^2 \rightarrow (2\pi^*)^2$ double excitations in the complex. Here we emphasize that (a) this excitation is of primary importance for describing the atomic promotion energy and (b) it must be computed carefully so the extra molecular correlation part is free of basis set superposition error.

From the theory of van der Waals complexes, the types of electron correlation giving rise to dispersion energy are well-understood. These involve correlation between electrons on different fragments and are described by simultaneous excitation of an electron to a different orbital in each of two fragments. Dispersion effects evaluated at the long bond lengths in van der

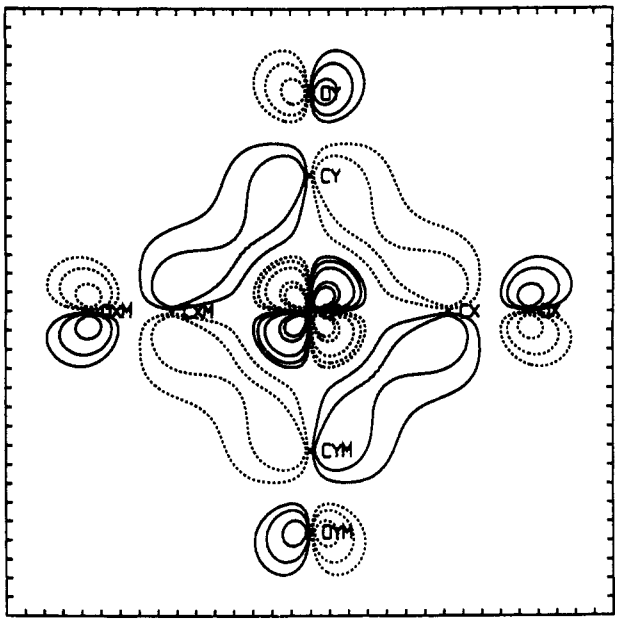

Figure 7. The $2\pi^*$ t_{2g} xy "empty" correlating orbital of $Cr(CO)_6$.

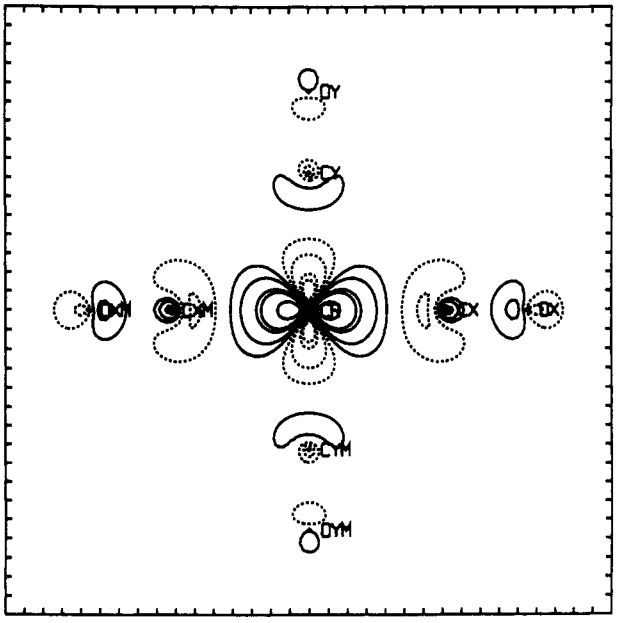

Figure 8. The 3d e_g $x^2 - y^2$ "empty" correlating orbital of $Cr(CO)_6$.

Waals complexes are small but behave like R^{-6}, so they can make a large contribution at shorter bond lengths. Dispersion effects of this type could account for a large fraction of the extra correlation energy.

Our calculations[9] show an unexpected large contribution involving a different type of excitation. In this excitation, electrons are moved from the metal 3d t_{2g} and the cage 5σ e_g orbitals to the cage $2\pi^*$ t_{2g} and metal 3d e_g empty orbitals shown in Figures 7 and 8. There are two independent ways to do this consistent with the correct total spin. One is the dispersion excitation just mentioned,

$$(3d\ t_{2g} \rightarrow 3d\ e_g)(5\sigma\ e_g \rightarrow 2\pi^*\ t_{2g}) \qquad (10)$$

which makes a small contribution. The other is the charge-transfer double replacement

$$(3d\ t_{2g} \rightarrow 2\pi^*\ t_{2g})(5\sigma\ e_g \rightarrow 3d\ e_g) \qquad (11)$$

The latter has a coefficient roughly proportioned to

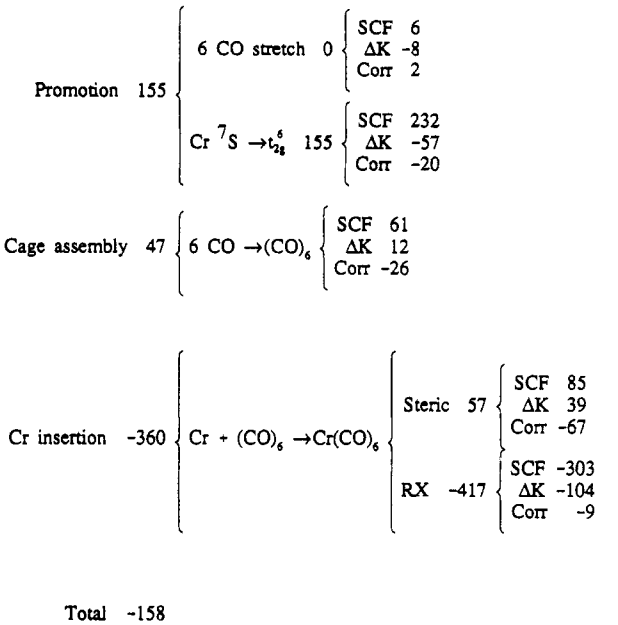

Figure 9. Energetics of various steps in $Cr(CO)_6$ formation (kcal/mol) from density functional calculations showing the difference ΔK from Hartree–Fock exchange and the estimated correlation correction.

the product of the $3d/2\pi^*$ and $5\sigma/3d$ overlap and so was expected by us to be small. In fact, it accounts for a large part of the extra molecular correlation energy. This describes a correlation in the electron positions so that, if the 5σ e_g electrons are closer than average to the chromium, the chromium 3d t_{2g} electrons are farther than average from the chromium and vice versa. If the expansion of the 3d t_{2g} orbital in the MO calculation is regarded as caused by static shielding by 5σ, then this correlation effect could be called dynamic shielding.

Hence the picture that emerges from this analysis is that the driving force for the bond is the electrostatic energy from the penetration of the 5σ electrons into the chromium valence shell. This penetration causes increased static shielding (resulting in increased diffuseness of 3d t_{2g} and π back-bonding) and dynamic shielding (resulting in strong correlation between the 5σ and 3d electron positions). Only when both static and dynamic shielding are considered are the energy-lowering terms sufficient to overcome the high promotion energy and the exchange repulsion from overlap of 5σ with the metal 3s and 3p core electrons.

It is interesting to compare this picture with the density functional model. If the same SCF charge density is used to evaluate the energy changes, the energy for each promotion and bonding step is roughly the same. In density functional theory, the molecular orbital exchange energy (not to be confused with the valence bond EX energy discussed above) differs from the SCF exchange energy, and the correlation energy with the best approximate equations also differs from the true correlation energy.[16] Due to extensive can-

(16) There are many approximate functionals in the literature. We have chosen to use the Becke gradient correction to the LDA exchange (Becke, A. D. *J. Chem. Phys.* **1988**, *88*, 2547) and the Perdew–Wang estimate of the correlation energy: (a) Perdew, J. P.; Wang, Y. *Phys. Rev. B* **1992**, *45*, 13244. (b) Perdew, J. P.; Chevary, J. A.; Vosko, S. H.; Jackson, K. A.; Pederson, M. R.; Singh, D. J.; Fiolhais, C. *Phys. Rev. B* **1992**, *46*, 6671. This combination of functionals was recently shown by Becke to produce accurate results for a variety of small test cases. Becke, A. D. *J. Chem. Phys.* **1992**, *97*, 9173.

cellation, however, the sum of the density functional excess exchange energy over the SCF value, ΔK, and the correlation energy comes close to the true correlation energy of the molecule. This is illustrated in Figure 9. The promotion steps have nearly the same value as found in Figure 2, but now the correction to the atomic promotion is ascribed to an incorrect estimate of K and a small correlation correction. The cage assembly also has a similar value in both figures (recall that the correlation part of this was lumped into the extra molecular correlation in Figure 2). During the insertion step, the density functional exchange energy again accounts for most of the difference from the SCF result. Thus the total bonding energy and the energy change for each physical step are similar in the two approaches, but the correlation effects in the ab initio calculation are mostly accounted for by a different estimate of the exchange energy in the density functional method.

Conclusion

This basic model of carbonyl bonding is consistent with all of the metal carbonyl molecules studied by us and others. It emphasizes the obvious fact that orbital changes are driven by electrical forces and the Pauli exclusion principle and not by overlap of basis functions. The "hardest" (least polarizable) orbitals are changed little but still contribute to the energy through electrostatic attraction made possible by penetration. The "softest" (most polarizable) orbitals respond by moving out of the way. This static polarization of the soft orbitals is essential to bonding and provides the most visible changes in electron density.

In order to obtain a qualitatively correct understanding of the bond energy, it is essential to consider the atomic promotion energy. This is a large number compared to the bond strength and is poorly estimated by Hartree–Fock theory. The extra molecular correlation energy is also approximately equal to the total bond energy. For $Cr(CO)_6$, this has been shown to be largely due to dynamic shielding described by charge-transfer double excitation in opposite directions.

F.B.C.M. expresses his gratitude to Conselho Nacional de Desenvolvimento Cientifico e Tecnologico (CNPq) of Brazil for financial support and to Instituto de Estudos Avançados for the opportunity to carry out postdoctoral research at Indiana University. This work was supported in part by a grant from the National Science Foundation.